Novel Eco-friendly Retrofitting Techniques for Dilapidated and Heritage Structures

Lead Guest Editor: Ravindran Gobinath
Guest Editors: Ganapathy GP and Isaac Ibukun Akinwumi

Novel Eco-friendly Retrofitting Techniques for Dilapidated and Heritage Structures

Novel Eco-friendly Retrofitting Techniques for Dilapidated and Heritage Structures

Lead Guest Editor: Ravindran Gobinath
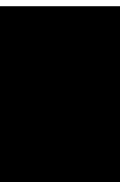Guest Editors: Ganapathy GP and Isaac Ibukun Akinwumi

Zhaofei Chu (iD), China
Wonseok Chung (iD), Republic of Korea
Donato Ciampa (iD), Italy
Gian Paolo Cimellaro, Italy
Francesco Colangelo, Italy
Romulus Costache (iD), Romania
Liviu-Adrian Cotfas (iD), Romania
Antonio Maria D'Altri, Italy
Bruno Dal Lago (iD), Italy
Amos Darko (iD), Hong Kong
Arka Jyoti Das (iD), India
Dario De Domenico (iD), Italy
Gianmarco De Felice (iD), Italy
Stefano De Miranda (iD), Italy
Maria T. De Risi (iD), Italy
Tayfun Dede, Turkey
Sadik O. Degertekin (iD), Turkey
Camelia Delcea (iD), Romania
Cristoforo Demartino, China
Giuseppe Di Filippo (iD), Italy
Luigi Di Sarno, Italy
Fabio Di Trapani (iD), Italy
Aboelkasim Diab (iD), Egypt
Thi My Dung Do, Vietnam
Giulio Dondi (iD), Italy
Jiangfeng Dong (iD), China
Chao Dou (iD), China
Mario D'Aniello (iD), Italy
Jingtao Du (iD), China
Ahmed Elghazouli, United Kingdom
Francesco Fabbrocino (iD), Italy
Flora Faleschini (iD), Italy
Dingqiang Fan, Hong Kong
Xueping Fan, China
Qian Fang (iD), China
Salar Farahmand-Tabar (iD), Iran
Ilenia Farina, Italy
Roberto Fedele, Italy
Guang-Liang Feng (iD), China
Luigi Fenu (iD), Italy
Tiago Ferreira (iD), Portugal
Marco Filippo Ferrotto, Italy
Antonio Formisano (iD), Italy
Guoyang Fu, Australia
Stefano Galassi (iD), Italy

Junfeng Gao (iD), China
Meng Gao (iD), China
Giovanni Garcea (iD), Italy
Enrique García-Macías, Spain
Emilio García-Taengua (iD), United Kingdom
DongDong Ge (iD), USA
Khaled Ghaedi, Malaysia
Khaled Ghaedi (iD), Malaysia
Gian Felice Giaccu, Italy
Agathoklis Giaralis (iD), United Kingdom
Ravindran Gobinath, India
Rodrigo Gonçalves, Portugal
Peilin Gong (iD), China
Belén González-Fonteboa (iD), Spain
Salvatore Grasso (iD), Italy
Fan Gu, USA
Erhan Güneyisi (iD), Turkey
Esra Mete Güneyisi, Turkey
Pingye Guo (iD), China
Ankit Gupta (iD), India
Federico Gusella (iD), Italy
Kemal Hacıefendioğlu, Turkey
Jianyong Han (iD), China
Song Han (iD), China
Asad Hanif (iD), Macau
Hadi Hasanzadehshooiili (iD), Canada
Mostafa Fahmi Hassanein, Egypt
Amir Ahmad Hedayat (iD), Iran
Khandaker Hossain (iD), Canada
Zahid Hossain (iD), USA
Chao Hou, China
Biao Hu, China
Jiang Hu (iD), China
Xiaodong Hu, China
Lei Huang (iD), China
Cun Hui (iD), China
Bon-Gang Hwang, Singapore
Jijo James (iD), India
Abbas Fadhil Jasim (iD), Iraq
Ahad Javanmardi (iD), China
Krishnan Prabhakan Jaya, India
Dong-Sheng Jeng (iD), Australia
Han-Yong Jeon, Republic of Korea
Pengjiao Jia, China
Shaohua Jiang (iD), China

Chayut Ngamkhanong (iD), Thailand
Trung Ngo, Australia
Tengfei Nian, China
Mehdi Nikoo (iD), Canada
Youjun Ning (iD), China
Olugbenga Timo Oladinrin (iD), United Kingdom
Oladimeji Benedict Olalusi, South Africa
Timothy O. Olawumi (iD), Hong Kong
Alejandro Orfila (iD), Spain
Maurizio Orlando (iD), Italy
Siti Aminah Osman, Malaysia
Walid Oueslati (iD), Tunisia
SUVASH PAUL (iD), Bangladesh
John-Paris Pantouvakis (iD), Greece
Fabrizio Paolacci (iD), Italy
Giuseppina Pappalardo (iD), Italy
Fulvio Parisi (iD), Italy
Dimitrios G. Pavlou (iD), Norway
Daniele Pellegrini (iD), Italy
Gatheeshgar Perampalam (iD), United Kingdom
Daniele Perrone (iD), Italy
Giuseppe Piccardo (iD), Italy
Vagelis Plevris (iD), Qatar
Andrea Pranno (iD), Italy
Adolfo Preciado (iD), Mexico
Chongchong Qi (iD), China
Yu Qian, USA
Ying Qin (iD), China
Giuseppe Quaranta (iD), Italy
Krishanu ROY (iD), New Zealand
Vlastimir Radonjanin, Serbia
Carlo Rainieri (iD), Italy
Rahul V. Ralegaonkar, India
Raizal Saifulnaz Muhammad Rashid, Malaysia
Alessandro Rasulo (iD), Italy
Chonghong Ren (iD), China
Qing-Xin Ren, China
Dimitris Rizos (iD), USA
Geoffrey W. Rodgers (iD), New Zealand
Pier Paolo Rossi, Italy
Nicola Ruggieri (iD), Italy
JUNLONG SHANG, Singapore

Nikhil Saboo, India
Anna Saetta, Italy
Juan Sagaseta (iD), United Kingdom
Timo Saksala, Finland
Mostafa Salari, Canada
Ginevra Salerno (iD), Italy
Evangelos J. Sapountzakis (iD), Greece
Vassilis Sarhosis (iD), United Kingdom
Navaratnarajah Sathiparan (iD), Sri Lanka
Fabrizio Scozzese (iD), Italy
Halil Sezen (iD), USA
Payam Shafigh (iD), Malaysia
M. Shahria Alam, Canada
Yi Shan, China
Hussein Sharaf, Iraq
Mostafa Sharifzadeh, Australia
Sanjay Kumar Shukla, Australia
Amir Si Larbi (iD), France
Okan Sirin (iD), Qatar
Piotr Smarzewski (iD), Poland
Francesca Sollecito (iD), Italy
Rui Song (iD), China
Tian-Yi Song, Australia
Flavio Stochino (iD), Italy
Mayank Sukhija (iD), USA
Piti Sukontasukkul (iD), Thailand
Jianping Sun, Singapore
Xiao Sun (iD), China
T. Tafsirojjaman (iD), Australia
Fujiao Tang (iD), China
Patrick W.C. Tang (iD), Australia
Zhi Cheng Tang (iD), China
Weerachart Tangchirapat (iD), Thailand
Xiaxin Tao, China
Piergiorgio Tataranni (iD), Italy
Elisabete Teixeira (iD), Portugal
Jorge Iván Tobón (iD), Colombia
Jing-Zhong Tong, China
Francesco Trentadue (iD), Italy
Antonello Troncone, Italy
Majbah Uddin (iD), USA
Tariq Umar (iD), United Kingdom
Muahmmad Usman, United Kingdom
Muhammad Usman (iD), Pakistan
Mucteba Uysal (iD), Turkey

Ilaria Venanzi (iD), Italy
Castorina S. Vieira (iD), Portugal
Valeria Vignali (iD), Italy
Claudia Vitone (iD), Italy
Liwei WEN (iD), China
Chunfeng Wan (iD), China
Hua-Ping Wan, China
Roman Wan-Wendner (iD), Austria
Chaohui Wang (iD), China
Hao Wang (iD), USA
Shiming Wang (iD), China
Wayne Yu Wang (iD), United Kingdom
Wen-Da Wang, China
Xing Wang (iD), China
Xiuling Wang (iD), China
Zhenjun Wang (iD), China
Xin-Jiang Wei (iD), China
Tao Wen (iD), China
Weiping Wen (iD), China
Lei Weng (iD), China
Chao Wu (iD), United Kingdom
Jiangyu Wu, China
Wangjie Wu (iD), China
Wenbing Wu (iD), China
Zhixing Xiao, China
Gang Xu, China
Jian Xu (iD), China
Panpan (iD), China
Rongchao Xu (iD), China
HE YONGLIANG, China
Michael Yam, Hong Kong
Hailu Yang (iD), China
Xu-Xu Yang (iD), China
Hui Yao (iD), China
Xinyu Ye (iD), China
Zhoujing Ye , China
Gürol Yildirim (iD), Turkey
Dawei Yin (iD), China
Doo-Yeol Yoo (iD), Republic of Korea
Zhanping You (iD), USA
Afshar A. Yousefi (iD), Iran
Xinbao Yu (iD), USA
Dongdong Yuan (iD), China
Geun Y. Yun (iD), Republic of Korea

Hyun-Do Yun (iD), Republic of Korea
Cemal YİĞİT (iD), Turkey
Paolo Zampieri, Italy
Giulio Zani (iD), Italy
Mariano Angelo Zanini (iD), Italy
Zhixiong Zeng (iD), Hong Kong
Mustafa Zeybek, Turkey
Henglong Zhang (iD), China
Jiupeng Zhang, China
Tingting Zhang (iD), China
Zengping Zhang, China
Zetian Zhang (iD), China
Zhigang Zhang (iD), China
Zhipeng Zhao (iD), Japan
Jun Zhao (iD), China
Annan Zhou (iD), Australia
Jia-wen Zhou (iD), China
Hai-Tao Zhu (iD), China
Peng Zhu (iD), China
QuanJie Zhu (iD), China
Wenjun Zhu (iD), China
Marco Zucca, Italy
Haoran Zuo, Australia
Junqing Zuo (iD), China
Robert Černý (iD), Czech Republic
Süleyman İpek (iD), Turkey

Contents

Hindawi

Research Article

Postfire Residual Strength and Morphology of Concrete Incorporating Natural Rubber Latex Exposed to Elevated Temperatures

Paul O. Awoyera ,[1] Hadee Mohammed Najm,[2] Olusegun David Adefarati,[1] Moutaz Mustafa A. Eldirderi,[3] Khaled Mohamed Khedher,[4,5] Husam Al Dughaishi ,[6] Jawad Al Lawati ,[6] and Abdalrhman Milad [6]

[1]*Department of Civil Engineering, Covenant University, Ota 112233, Nigeria*
[2]*Department of Civil Engineering, Bilad Alrafidain University College, Diyala 32001, Iraq*
[3]*Department of Chemical Engineering, College of Engineering, King Khalid University, Abha 61421, Saudi Arabia*
[4]*Department of Civil Engineering, College of Engineering, King Khalid University, Abha 61421, Saudi Arabia*
[5]*Department of Civil Engineering, High Institute of Technological Studies, Mrezga University Campus, Nabeul 8000, Tunisia*
[6]*Department of Civil and Environmental Engineering, College of Engineering, University of Nizwa, P.O. Box 33, Nizwa PC 616, Ad-Dakhiliyah, Oman*

Correspondence should be addressed to Paul O. Awoyera; paul.awoyera@covenantuniversity.edu.ng

The exposure of concrete to elevated temperatures is known to cause diverse severe damages in concrete composites. Hence, measures to improve the performance of concrete during exposure to fire are continually proposed. The present study investigated the postfire residual strength and morphology of concrete incorporating natural rubber latex exposed to elevated temperature. Four different concrete mixes were considered for the investigation, namely, a control sample made without natural rubber latex, the second sample containing 1% natural rubber latex, the third sample containing 1.5% natural rubber latex, and the fourth sample containing 3% of natural rubber latex. The concrete samples (150 mm cubes and 100×200 mm cylinders) were exposed to varying temperatures 300°C, 800°C, and 1000°C, after the curing process. Nondestructive tests using Schmidt rebound hammer and ultrasonic pulse tester were carried out on samples. The compressive strength and split-tensile strength of concrete cubes and cylinders, respectively, were determined. Micrographs and elemental distribution in the sample were studied using the scanning electron microscopy (SEM-EDX) apparatus. It could be seen from the results that the concrete strength properties reduced as the exposure temperature increased. The results also showed that NRL could be sparingly utilized as a concrete admixture, at 1% content. The performance of concrete was not stable at over 300°C when NRL addition was above 1%.

1. Introduction

For several years, mortar and concrete have been widely considered as construction materials because of many factors such as economic benefits and structural performance. Portland cement and concrete possess deficiencies that can affect their usages such as their low tensile strength, delayed hardening, large drying shrinkage, low resistance against chemical attacks, and elevated temperature. Several cases of fire accidents in concrete structures recorded around the world are alarming; thus, finding ways to enhance concrete matrix to ensure adequate fire resistance is the key motivation for this research. However, to reduce the deficiencies of these materials, there have been various attempts at the

use of admixtures in the modification of the concrete mixtures. An example of the admixture is natural rubber latex. The attempt to use polymer-modified cement or concrete involves the alteration of ordinary Portland cement or concrete with polymer additives. Examples include latexes, water-soluble polymers, redispersible polymer powder, liquid-resins, and monomers [1].

From tests carried out by researchers, it has been made known that cement concrete is poor in terms of heat conductivity but can sustain considerable damages, which can affect its integrity in terms of strength and other mechanical properties when exposed to fire for an extended period. As part of a post-fire evaluation of concrete, the forensic expert would require to know the history of fire exposure for cement concrete, in terms of the duration of fire and exposure condition. Overall, it helps to figure out the extent of damage to concrete structures and other components and to ascertain if the materials are structurally sound. Such assessments of fire damage to concrete structures start with the visual observation of color change, checking the occurrence of spalling on the concrete [2].

As a result, natural and synthetic polymers were first included in concrete and mortar mixes in the twentieth century. Since then, there has been a significant and noticeable increase in both natural and synthetic polymers [3]. Polymers are being incorporated widely at an increasing rate in civil engineering and other uses as modifiers, especially in improving the general service performance of both cement concrete and mortar [4, 5].

Indeed, polymer-modified cement concrete and mortar are now widely used as both finishes and corrective materials on cement concrete as well as masonry work, due to already known facts that the applications of these materials involve placement of the materials on surface positions. Therefore, the material is very much likely to receive the first-degree impact in the event of thermal and fire attack [4].

Research studies have shown that natural rubber latex (NRL) displays superior properties over other known elastomeric latexes, most importantly in the field of application of high performance that would inquire on the excellent mechanical properties such as the property of high tensile strength and resilience as well as abrasion resistance of the natural material [3].

Years back, the resistance of polymer cement concrete and mortar was considered low mainly because of the thermal instability, and another known cause is adherent combustibility. Efforts are directed towards the prevention of failure due to the low thermal ability of polymer cement concrete and mortar from the use of vermiculites-a material that can be substituted for normal aggregate due to its low thermal conductivity, to the limitation of adding latex contents to a cement concrete and mortar mixtures [4].

The addition of polymers in cement and aggregate acts as modified cement concrete, which has been shown to have effective results compared to that of conventional concrete. The addition of the polymer has effects on improved workability, tensile strength, bond strength, and fire resistivity on cement concrete and mortar. A layer is formed on the cement and aggregate by the polymer, which makes the cement concrete to be less permeable and consequently causing a reduction in the moisture retention corrosion and environmental attacks on the concrete [1].

Subash et al. [6] reported that polymers have long chain structures resulting in a developed long-range network structure of bonding, which thus influenced an improvement in the flexural strength of natural rubber latex modified concrete. Generally, the use of normal concrete (NC) has significantly changed over the years. There is the quest for improvement of the physical, mechanical, and chemical properties of normal concrete (NC). The current study explored the use of natural polymers to increase the fire resistance of normal concrete.

Natural rubber latex-based concrete has been shown to improve on some of those shortcomings depending on the water-latex% ratio and grade of concrete used.

Natural rubber latex is a product formed naturally from the "Hevea Brasiliense's tree" also known as "Para rubber tree" which is mostly found in countries such as Malaysia, Brazil, Sri Lanka, India, and Indonesia and is formed as a result of polymerization of isoprene (C_5H_8) or the loosely joining of the monomers of isoprene (C_5H_8) in the shape of a long-tangled chain. Natural rubber latex is an environmental friendly water-based colloidal dispersion of rubber particles (RPs) [7].

In the fourth millennium B.C., asphalt, a natural polymer, was used in the mortar of the clay brick walls of Babylon. Mortar made from 25–35% bitumen (a natural polymer), loam, and chopped straw or reeds was used to lay the masonry foundations for the temple of Ur-Nina (King of Lagash) at Kish [1]. The natural rubber latex (NRL) was used in the concrete to serve as an admixture; it was stirred with the mixing water to be used for the dry component mix (it is the mixture of ingredients Portland cement, coarse aggregate, water, fine aggregate, and NRL), homogeneously.

The inferior quality exhibited by concrete when exposed to aggressive environments such as fire and chemical attacks, is a major concern to concrete users. Therefore, it is very necessary for other improvement schemes to be adopted during concrete production. Various admixtures are used to enhance the performance of concrete, but the majority of these admixtures are synthetic, and are sourced at a high cost. However, the current study utilizes natural rubber latex to enhance the post-fire properties of concrete. The rubber latex can be extracted from rubber trees in areas where it is dominant; at a low cost.

The objective of the present study is to assess the effect of natural rubber latex on the fire resistance of normal concrete, as well as to characterize the properties of natural rubber latex-induced concrete, and furthermore ascertain the optimum natural rubber latex% for improvement in the fire resistance of concrete.

The literature have covered many existing experimental works that evaluate the behaviour of concrete exposed to elevated temperatures and tested under destructive and nondestructive loadings [8]. However, there is no available experimental work to evaluate the effect of natural rubber latex as admixture materials in concrete on the workability, mechanical, microstructural, and fire-resistance

characteristics, which is important to investigate under destructive (compressive and tensile) and nondestructive (rebound hammer test and ultrasonic pulse velocity test) loadings. The obtained data from this study can be used as a reference for future studies and provide extensive data for natural rubber latex studies.

2. Materials and Methods

The materials used to prepare the concrete mix design, concrete specimens, and tests on the fresh and hardened concrete are described in this section. The study compares the fire resistivity of natural rubber latex concrete with conventional concrete. The mechanical and morphology properties of concrete are evaluated following exposure of the samples to fire. A flowchart for the research process is shown in Figure 1(a).

2.1. Materials. The binding material used in this study is grade 42.5 Ordinary Portland cement. It is a type I multifunctional cement that meets ASTM C150 [9] requirements; no preliminary test was carried out on the cement. Table 1 shows the oxide composition and physical properties of the cement used.

The fine aggregate used in this study was sharp sand, passing through a 4.75 mm sieve, obtained from Ota, Ogun state, Nigeria. Granite, crushed natural stone, was used as coarse aggregate in this research work. The aggregate sizes are not exceeding 12.5 mm. The water utilized in this research is sourced from the municipal water supply of the civil engineering building of Covenant University Ota, Ogun State, Nigeria.

Rubber latex was utilized in this research work as an admixture (Figure 1(b)). It was sourced from Ota, Ogun state Nigeria. Table 2 shows the chemical analysis of natural rubber latex.

Table 3 shows the concrete mixes considered in this study.

2.2. Batching and Mixing of Constituents. Batching is the method of measuring and mixing concrete components by the mix design. This procedure can be carried out in two ways: by volume or by weight. In this research work, the batching was carried out by weight (see Table 4). Natural rubber latex was added in ratio to the total volume of the sample at different percentages; it was added at 1%, 1.5%, and 2%.

The mix ratio used for this study was ratio $1 : 1.5 : 3$, with a concrete grade of $25 \, \text{N/mm}^2$, and the water-to-cement ratio is 0.47. The mixing of concrete constituents was carried out manually. The dry constituents were first mixed till uniform distribution was attained. The natural rubber latex was mixed with the portable water and gradually added to obtain a thorough and workable mix. The casting takes place immediately after the mixing is completed and in-situ tests have been carried out on the fresh concrete. Four different concrete specimens were produced for examination in this study: the first control sample is without natural rubber latex, the second sample contains 1% of natural rubber latex, the third sample contains 1.5% of natural rubber latex, and the fourth sample contains 3% of natural rubber latex.

2.3. Preliminary Test on Aggregate and Cement

2.3.1. Aggregate Impact Test. This test is a deciding factor in assessing the resistance of a coarse aggregate to abrupt impact or shock, and the test also provides as to how much impact load aggregate can withstand as aggregate should be tough enough to resist disintegration due to impact. Table 5 presents the calculations for the aggregate impact value.

$$\text{Calculation for sample 1,}$$
$$W_1 = 557 - 185 = 372 \text{g,}$$
$$\text{Impact value} = W_2/W_1 \times 100 \quad (1)$$
$$= 75/372$$
$$= 0.2016 \times 100 = 20.16\%.$$

2.3.2. Specific Gravity Test. Specific gravity represents the mass of a substance divided by the quantity of water in the same amount of substance. The specific gravity for the cement used was determined as presented in Table 6.

$$GS_A = \frac{Wo}{Wo + (WA - WB)} = \frac{168}{168 + (-104)} = 2.65,$$

$$GS_B = \frac{Wo}{Wo + (WA - WB)} = \frac{168}{168 + (-96)} = 2.33,$$

$$GS_g = \frac{2.625}{2.33} = 1.12,$$

$$(2)$$

The specific gravity for sand $= 1.12$.

(a)   (b)
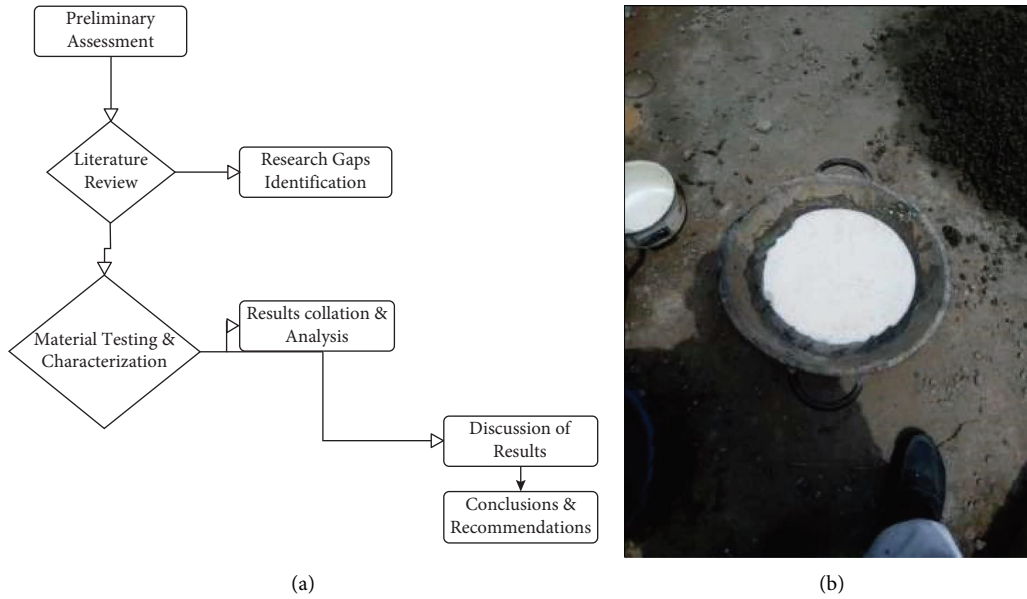
Figure 1: (a) Research process flowchart. (b) Natural rubber latex.

Table 1: Oxide composition and physical properties of cement used.

Chemical analysis		Physical analysis	
Oxide composition	Percentage by weight (%)	Property	Magnitude
K_2O	0.46	Moisture content (%)	2.4
MgO	1.25	Specific gravity	3.15
Fe_2O_3	4.301	Bulk density (g/cm^3)	2.95
SiO_2	53.2	Fineness modulus	0.88
CaO	11.52	pH	8.8
Al_2O_3	21.4		
Na_2O	1.04		
Loss on ignition	6.78		

Table 2: Chemical analysis of natural rubber latex.

Property	TSC%	DRC%	NRC%	pH	VFA%	NH_3%	MST (s)	Specie
Magnitude	61.64	60.09	1.45	10.07	0.018	0.25	1227	Multiple

Table 3: Sample labelling.

S/N	Sample	Proportions
1	Control sample	Control sample containing no NRL
2	M1	Sample containing 1% of NRL
3	M2	Sample containing 1.5% of NRL
4	M3	Sample containing 3% of NRL

Table 4: Concrete mix design.

Concrete specimen	Cement (kg)	Fine aggregate (kg)	Coarse aggregate (kg)	Water (kg)	Natural rubber latex (%)	Natural rubber latex (kg)
Control sample	1.50	2.25	4.5	0.73	0	0.00
M1	1.50	2.25	4.5	0.73	1	0.015
M2	1.50	2.25	4.5	0.73	1.5	0.023
M3	1.50	2.25	4.5	0.73	2	0.03

TABLE 5: Aggregate impact test value.

Sample	1
Weight of calibrated cylinder (g)	185
Weight of sample + cylinder (g)	557
W_1 = weight of sample (g)	372
Weight of sample passing through 2.36, sieve (W_2)	75
Impact value (%)	20.16

TABLE 6: Specific gravity values of fine aggregate.

Sample	A	B
W_p = mass of empty bottle (g)	154.0	151.0
W_{Ps} = mass of bottle of sample (g)	322.0	319.0
W_B = mass of bottle + sample + water (g)	553.0	544.0
W_A = mass of bottle water (g)	449.0	448.0
$W_O = W_{Ps} - W_p$	168.0	168.0

2.4. Test on Fresh Concrete

2.4.1. Slump Test. This test was carried out on concrete to measure the concrete sample's workability or fluidity in its fresh state. It is a method of determining the consistency or stiffness of concrete in an indirect manner.

2.5. Curing Method Adopted.
Curing of concrete fully controls the hydration process in the mixture [10]. Curing entails regulating the loss of moisture and, in certain cases, temperature. Curing techniques include membrane curing, steam curing, ponding technique, steam curing, immersion in water, shade concrete work, covering concrete surfaces with hessian or gunny bags, and spraying water [11].

In this study, the curing of concrete samples was performed by total immersion in water (Figure 2). Curing of cementitious matrix by immersion in water satisfies all requirements of curing, including the promotion of hydration, the elimination of shrinkage, and the absorption of heat of hydration.

2.6. Mechanical Property Test on Hardened Concrete

2.6.1. Compressive Strength. The compressive strength of concrete is a metric used to evaluate the material's resilience in the face of compressive stresses. It is a measurement of the concrete's resistance to failure when subjected to compressive pressures. The compressive strength of the concrete sample is determined by the division of the load applied at the point of failure with the cross-sectional area of the hardened concrete sample. Concrete cubes of 150 mm sizes were cast for the compressive strength test. Triplicate samples were tested, and the average result was noted for each of the mixes.

The samples were tested after 28 days of curing, and after they were exposed to varying temperatures 300°C, 800°C, and 1000°C, using a compressive strength machine (Figure 3).

FIGURE 2: Curing of concrete samples in the water tank.

2.6.2. Split Tensile Test. Due to the loading and specimen shape simplicity, the splitting tensile test is the most popular laboratory test for determining the tensile strength of concrete. This test involves delivering a distributed compressive force along the length of a concrete cylinder, giving rise to tensile stress formed perpendicular to the loading plane of the specimen's cross-section and sharp compressive stress around the load application spots [12]. Concrete cylinders of 100×200 mm sizes were cast for the split-tensile strength test. The samples were cured in water for 28 days prior to subjecting the materials to heating, and strength evaluation using the compressive strength machine displayed in Figure 3.

2.6.3. Microstructural Analysis Test

(1) Scanning Electron Microscopy (SEM). Scanning electron microscopy (Figure 4) is used for examining and scanning the surface of the material with a focused beam of electrons, through image analysis, to measure and assess fine details. When the electrons contacts atoms in the sample, they produce a variety of signals that provide information about the sample's surface topography and composition; SEM makes provision to investigate component failures, detect particles, and analyze the interactions between substances and substrates [13, 14].

2.6.4. Fire Resistance Test. Fire resistance is a measure of the ability of a material to resist the actions of fire and continue to fulfil its function over a measured period. This test was carried out to determine the resistivity of the concrete

FIGURE 3: Compressive strength machine.

FIGURE 4: Scanning electron microscope equipment.

specimens to fire at various temperatures. The industrial furnace is used for this procedure (Figure 5(a)), the desired temperature is from 300°C to 1000°C, and the maximum temperature output of the furnace is 1300°C. The cooling process employed for the sample after the heating process is complete is the pouring of water from a bowl unto the samples (Figure 5(b)).

2.6.5. Rebound Hammer Test. The rebound hammer test is considered to be a nondestructive concrete testing method that provides a practical and quick assessment of the concrete's compressive strength. The rebound hammer, also commonly known as the Schmidt hammer, is made out of a spring-loaded mass that slides along a plunger within a tubular casing.

The Schmidt hammer strikes the surface of the concrete with a set amount of force, and produces the rebound number, which is measured with the use of a meter; the rebound number measured from the meter is then compared with the compressive strength of the concrete (see Figures 6(a) and 6(b)).

2.6.6. Ultrasonic Pulse Velocity Test. As per the IS: 13311 (Part 1) [15] ultrasonic pulse velocity test is used to examine the condition of concrete by transmitting ultrasonic pulse to the concrete mass. The concrete ultrasonic test method is a nondestructive method of determining the homogeneity and durability of concrete (Figures 7(a) and 7(b)). Obtaining a higher UPV value or shorter pulse travel time implies that

(a)

(b)

FIGURE 5: (a) Heating of concrete in an industrial furnace. (b) Cooling process of concrete.

(a)

(b)

FIGURE 6: (a) Rebound hammer test on the hardened concrete cube. (b) Rebound hammer test on the hardened concrete cylinder.

(a)   (b)

FIGURE 7: Ultrasonic pulse velocity test on hardened concrete cube and cylinder.

the quality of concrete is adequate in terms of density, uniformity, and homogeneity, among other factors. The apparatus used for this test include the following:

(1) Amplifier

(2) Timing device

(3) Transducer

(4) Electrical pulse generator

3. Results and Discussions

This section presents a comprehensive overview of the data obtained, as well as its analysis and commentary. The objective of this section is to evaluate the results in order to infer additional information and effectively explain the study findings.

The findings of all the tests, including fresh and hardened concrete samples, are presented and analyzed in this section. Several tests were conducted on fresh and hardened concrete samples in order to assess the samples' overall performance, the mechanical, workability, and durability results are analyzed and discussed.

3.1. Fresh Concrete Test

3.1.1. Slump Test. Figure 8 represents the results of the slump test carried out immediately after mixing is
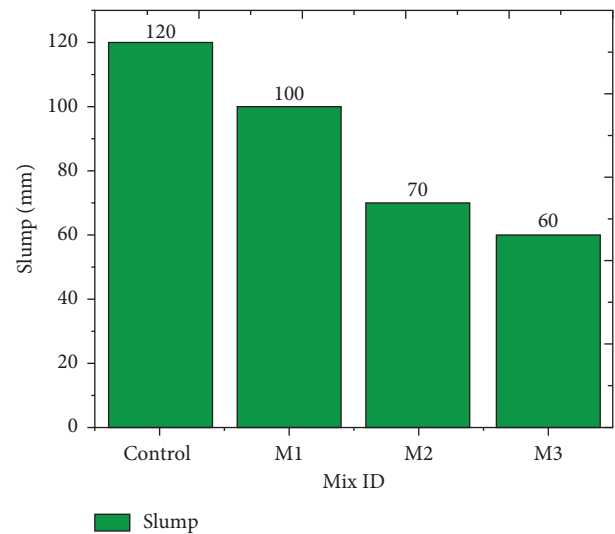
FIGURE 8: Slump test values of concrete samples.

performed; the slump test is carried out on the fresh concrete to determine the effects of NRL, at different percentages, on the workability of the fresh concrete. The slump value decreased with an increasing NRL value. In other words, increasing the addition of NRL content made the concrete to be more viscous; the NRL fills the pores and voids in the concrete in its fresh state turning the concrete into a solid

paste and decreasing its flow. The NRL particle present in the concrete mix decreases the fluidity of the mix; the dried NRL particles in the polymer occupy the pores in the mix and prevent the concrete from slumping [6]. According to Ismail et al. [5] it was shown that rapid setting of latex occurs, and this produces weak chains that steadily gain enough strength, this prevents the mix from achieving the requisite homogeneity when applied, and this appears to lower the amount of mixing water used by trapping part of it in its spongy interstices.

3.2. Hardened Concrete Test

3.2.1. Rebound Hammer Test.
The rebound number of concrete samples at varying temperatures is shown in Figure 9. The concrete samples in relation to the rebound number obtained from the Schmidt hammer are presented as follows.

At 300°C, M3 containing 2% NRL recorded the highest rebound number, 5% higher than the control sample containing no NRL at all. At this temperature, the control sample has the lowest record of the rebound number of 16, indicating that the quality of the sample after its subjection to fire is very poor, other samples M1, M2, and M3 accounted for rebound numbers well above 20; this connotes their quality to be superior to the control sample. At 800°C, there is an increase in the rebound number of all concrete samples/specimens apart from the M1 where a significant decrease in the rebound number is noted.

At 1000°C, the highest rebound number of 28 was obtained for Mix M1 containing 1% NRL. It could be deduced that the hammer number increased with increasing temperature upto 1000°C. Also, it implied that the concrete was completely dried and solidified with higher exposure temperature. A slightly higher hammer number was obtained for concrete containing NRL than the control mixture. The rebound number value of 28 obtained from M1 at 1000°C indicates that the concrete sample is fair in terms of quality, while that of the control sample, which has the lowest rebound number of 16 recorded in this experiment indicates that the quality of the control sample at that temperature is inferior to other samples in terms of quality. The description of the rebound hammer number was based on the standard stated by previous studies [16–18].

The data gotten from each concrete sample containing NRL presents itself to be incoherent and inconsistent, possibly due to the inclusion of the polymer additive at different percentages, as compared to the control sample, which has more progressive data. At 1000°C, a significant rise in the rebound number value is recorded in all concrete specimens; this could likely be attributed to the carbonation of concrete and the conditions as to which the specimens were stored before and after being subjected to the heating process.

3.2.2. Effect of Elevated Temperature on Rebound Number.
The results showed that the rebound hammer number increased with increasing temperature upto 1000°C. Concrete
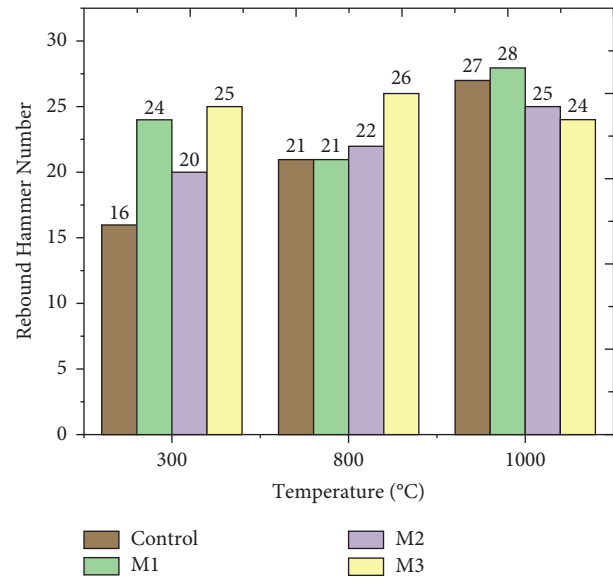

FIGURE 9: Rebound number of concrete samples at varying temperatures.

subjected to high temperature initially becomes stronger due to the expulsion of moisture, the value provided by the rebound hammer is a rough estimate based on the hardened surface of the concrete. Thus, the hammer number may not necessarily provide an in-depth of the actual strength of the concrete [16]. According to Kumavat et al. [17], the rebound hammer number of concretes increase with an increase in temperature from 200°C–400°C, it was also noted in their research that the rebound number was significantly higher than the compressive strength.

3.2.3. Ultrasonic Pulse Velocity of Concrete Cube.
In all concrete samples, the ultrasonic pulse velocity decreases as the damage caused by the elevating temperature increases. The control sample has the highest velocity at 300°C followed by the velocity of the M3 concrete sample still at 300°C. At 800°C, the damage caused by the increase in temperature causes the velocity for each sample to decrease, the control sample having the highest velocity of 3.6 km/s followed M2 concrete sample having the lowest velocity of 2.6 km/s. At 1000°C, the damage caused by the fire exposure is quite extensive, the control sample has the highest velocity of 2.9 km/s followed by M3 having the lowest velocity of 1.3 km/s. The low velocity recorded at 1000°C indicates that the quality M3 sample is doubtful. The control sample containing 0% NRL performs well overall in this non-destructive test. From Figure 10, it can be seen that with the increase in NRL%, the decrease in velocity occurs rapidly, which is more visible in the M3 concrete cube sample, as compared to that of the control sample.

3.2.4. Compressive Strength Test.
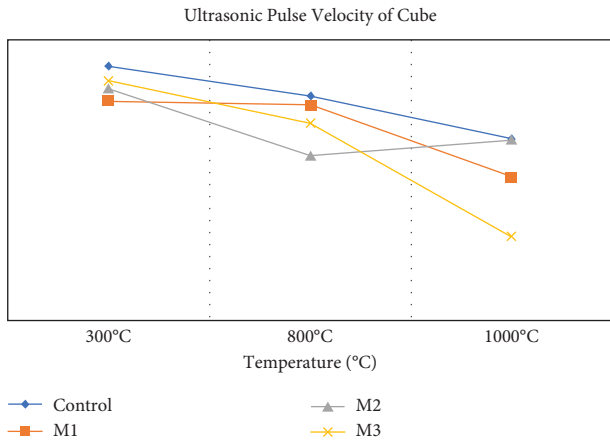Figure 11 shows the compressive strength values of the concrete samples.

FIGURE 10: Ultrasonic pulse velocity of concrete samples at varying temperatures.

$$\text{Compressive strength} = \frac{\text{Load value at failure}}{\text{Cross sectional area}},$$

$$\text{Area of cube mold} = 150\text{mm} \times 150\text{mm} = 22500\text{mm}^2.$$

$$(3)$$

At 31 N/mm^2, the control sample had the highest compressive strength at 7 days and was 44.5% higher than the M3 sample, which had the lowest compressive strength at 7 days at 17.8 N/mm^2. Across all samples, compressive strength at 7 days ranged from 17.8 N/mm^2 to 31 N/mm^2, compressive strength at 14 days ranged from 21 N/mm^2 to 36 N/mm^2, and compressive strength at 28 days ranged from 23.8 N/mm^2 to 23.8 N/mm^2 to 44 N/mm^2. At 44 N/mm^2, the control sample had the highest compressive strength and was 36.4% higher than the M3 sample, which had the lowest compressive strength of 23.8 N/mm^2 at 28 days.

3.2.5. Effects of NRL% on the Compressive Strength of Concrete without Heating. It could be observed from Figure 11 that based on the percentage quantity added, the inclusion of NRL contributed to the compressive strength of the concrete samples. Although the control sample performed best overall than the other samples but from the mix samples containing NRL, M2 containing 1.5% NRL gave higher values of compressive strength among others. In this study, the optimum dosage of NRL in quantity is 1.5%, and beyond that proved to only contribute to the decrease in compressive strength. To support the findings of this study according to Ismail et al [5] it was pointed out that the optimum dosage of NRL percentage for concrete is about 1.4% and at this percentage there was a 4.5% increase in strength of the mix containing NRL over that of normal concrete.

3.2.6. Compressive Strength at Elevated Temperature. The results of the compressive strength test after the heating process of the concrete samples at different levels of temperature are shown in Figure 12. The effect of the increasing temperature appears to have resulted in a continuous decrease in compressive strength in the different concrete
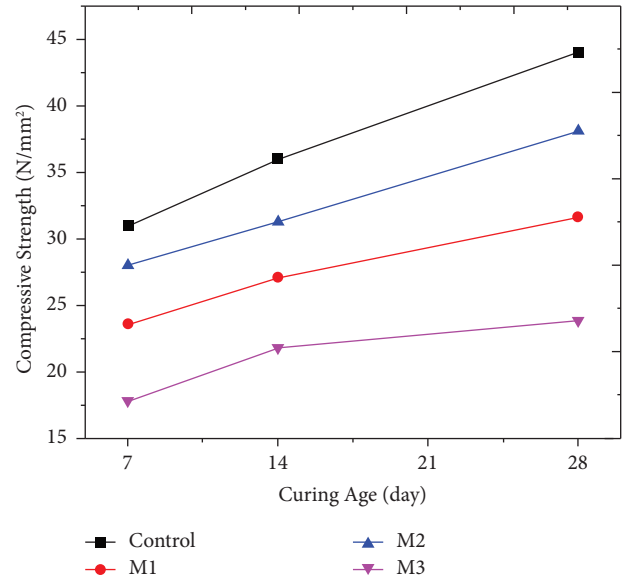

FIGURE 11: Compressive strength of concrete samples at different curing days.
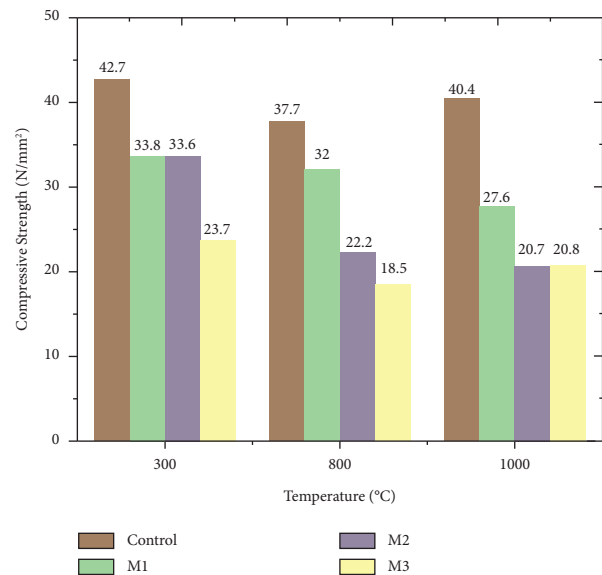

FIGURE 12: Compressive strength of concrete samples at varying temperatures.

samples. From the result the sample that does best is the control sample containing 0% NRL, it maintains a steady lead in compressive strength at the different levels of temperature indicating its superiority over M1, M2, and M3 concrete samples. At 300°C and with a compressive strength of 42.7 N/mm^2, the control sample has the highest compressive strength overall in all the samples followed by M3 having a compressive strength of 23.7 N/mm^2 presenting itself to be the lowest in compressive strength. At 800°C, the control sample performs best over the other samples with a compressive strength of 37.7 N/mm^2, and the concrete sample with the lowest compressive strength of 18.5 N/mm^2 is the M3 concrete sample. At 1000°C, the significant loss of

Compressive Vs Rebound (Control)

Compressive Strenght (MPa)

Compress Vs Rebound (M1)

Compressive Strength (MPa)

(a)

(b)

Compress Vs Rebound (M2)

Compressive Strenght (MPa)

Compressm Vs Rebound (M3)
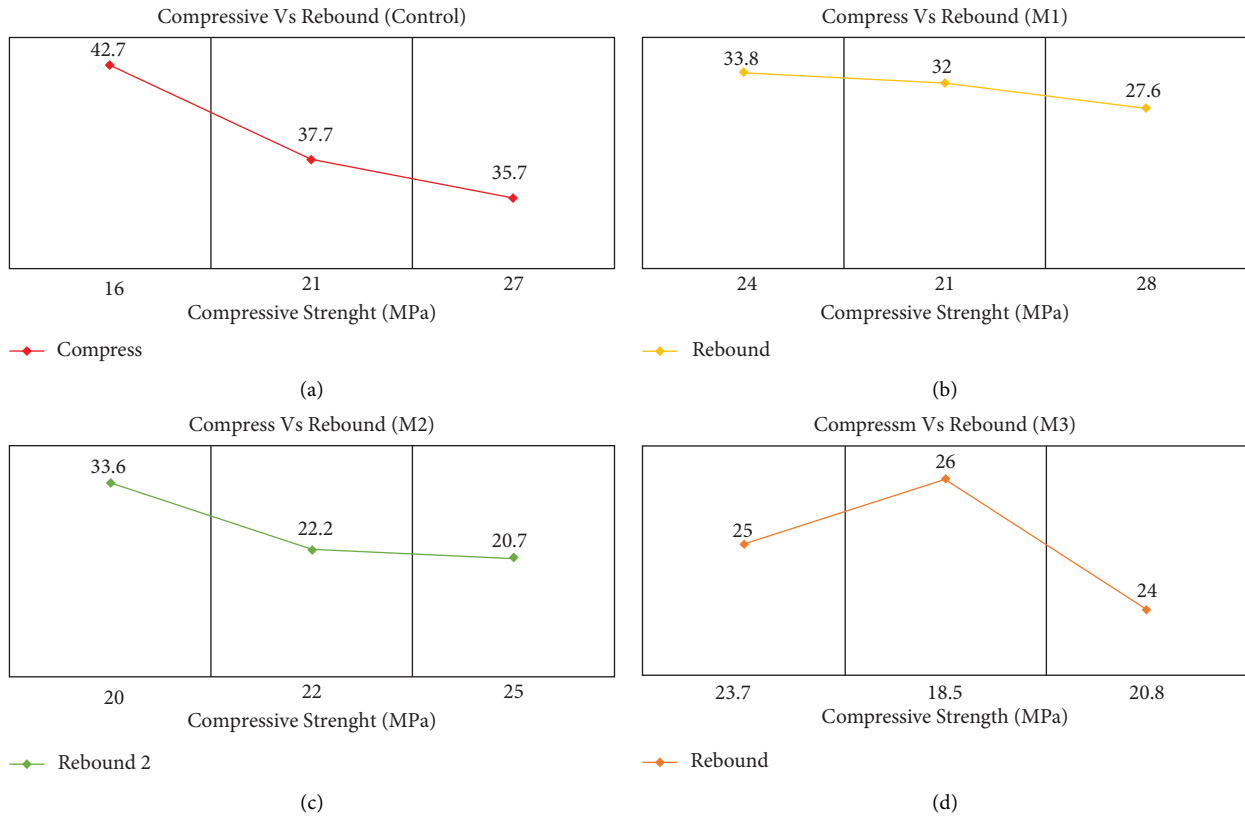
Compressive Strength (MPa)

(c)

(d)

FIGURE 13: (a–d) Relationship between concrete cube compressive strength and rebound hammer.

compressive strength is noted in M3 concrete sample; this implies that the increasing % of NRL in the concrete mix lowers the compressive strength of concrete, and its further declines with an increase in temperature. Generally, the decrease in compressive strength of the concrete sample post-fire exposure is attributed to the change in structure and breakdown of the concrete at a microstructural level during the heating process. A related study [5] also reported that in the process of heating, certain complex reactions such as shrinkage, breakdown, expansion, and crystal disintegration take place.

3.2.7. Effects of NRL% on the Compressive Strength. Figure 13 shows the relationship between concrete cube compressive strength and rebound hammer. Although the control sample performed best overall than the other samples from the mix samples containing NRL, however, M1 containing 1% NRL gave higher values of compressive strength, among others. In this study, the optimum dosage of NRL in quantity is 1%, and beyond that proved to only contribute to the decrease in compressive strength. This inferior performance of concrete strength observed as NRL was increased has been noted in similar tests [19–22].

3.2.8. Relationship between Rebound Number and Compressive Strength of Concrete. The relationship between rebound number and conpressive strength of concrete is as follows:
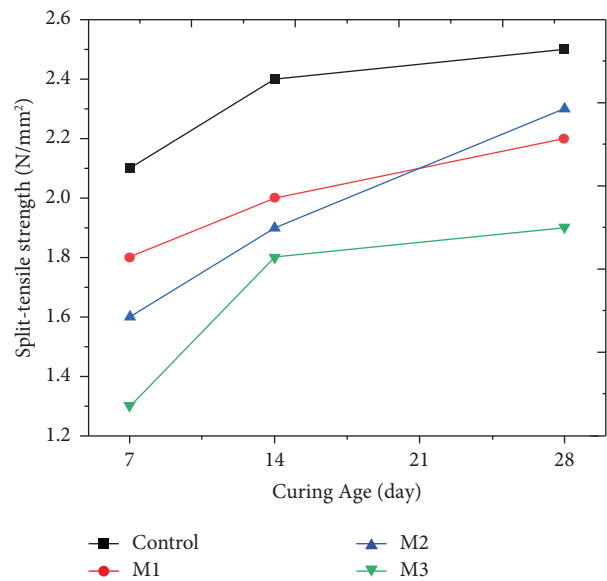

FIGURE 14: Split tensile strength for different curing days.

(a) Control sample

(b) M1 sample

(c) M2 sample

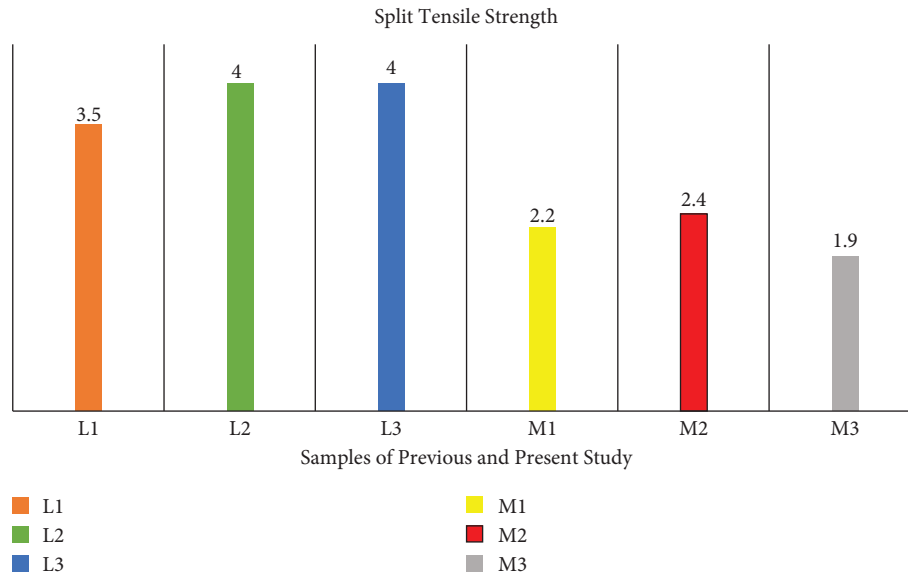(d) M3 sample

Split Tensile Strength

FIGURE 15: Comparison of split tensile strength between Subash et al. [6] and the present study.
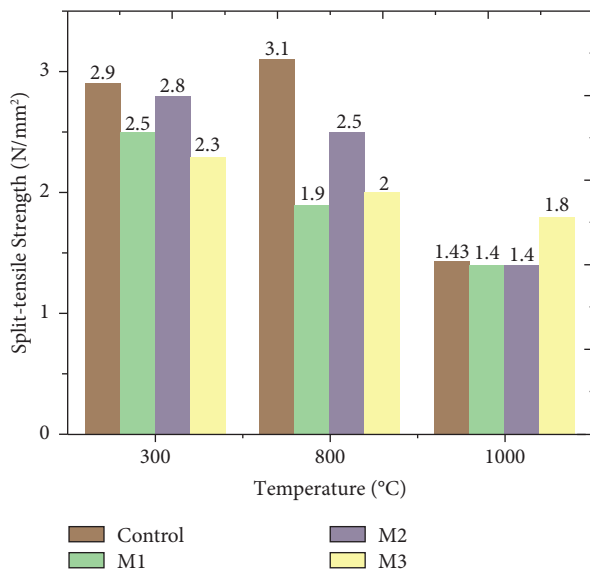

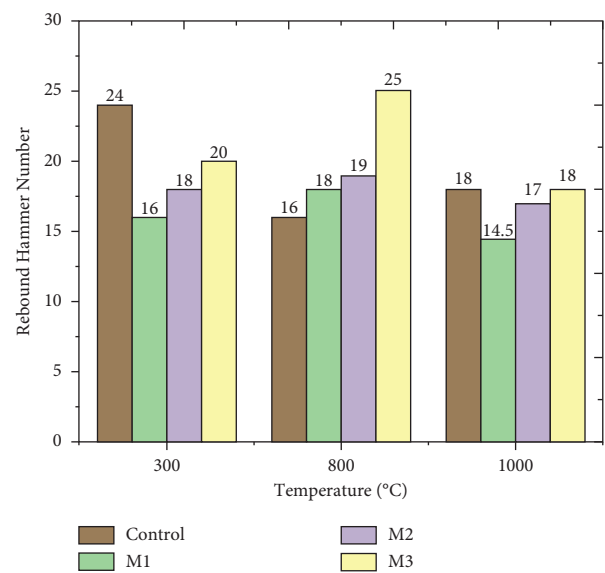FIGURE 16: Split tensile strength of postheated concrete.

FIGURE 17: Rebound number value of postheated concrete cylinder samples.

3.2.9. Split Tensile Strength Test. Figure 14 shows the split tensile strength values of the concrete samples.

$$\text{Split Tensile Strength}, T = \frac{2P}{\pi LD}, \tag{4}$$

where $T =$ splitting tensile strength (N/mm^2), $P =$ maximum applied load indicated by the testing machine (N), $L =$ average sample length in (mm), and $D =$ sample diameter in (mm).

Figure 14 presents the values gotten from the split tensile strength test of the concrete samples over different curing days. As early as 7 days the split tensile strength of the control sample appears to be the highest with a strength value of 2.1 N/mm^2 and is 34.9% higher than M3 with the lowest split tensile strength of 1.3 N/mm^2. Across all samples, split tensile strength at 7 days ranged from 1.3 N/mm^2 to 2.1 N/mm^2, and split tensile strength at 14 days ranged from 1.8 N/mm^2 to 2.4 N/mm^2. At 28 days of curing, the control sample had the highest split tensile strength of 2.5 N/mm^2 and was 28.4% higher than M3 with the lowest split tensile strength of 1.9 N/mm^2.

The control sample performs best overall than all the other samples, M1, M2, and M3; the split tensile strength trend line shows the order of highest to lowest split tensile strength, which follows from the control sample to the M1 sample to the M2 sample and then to M3 sample. The strength trend flow line implies that with the inclusion of NRL into the concrete mix, the split strength of the samples decreases.
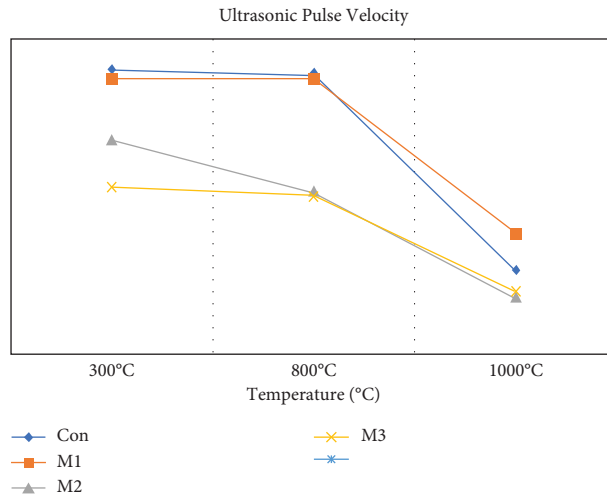
FIGURE 18: Ultrasonic pulse velocity test of postheated concrete cylinder samples.
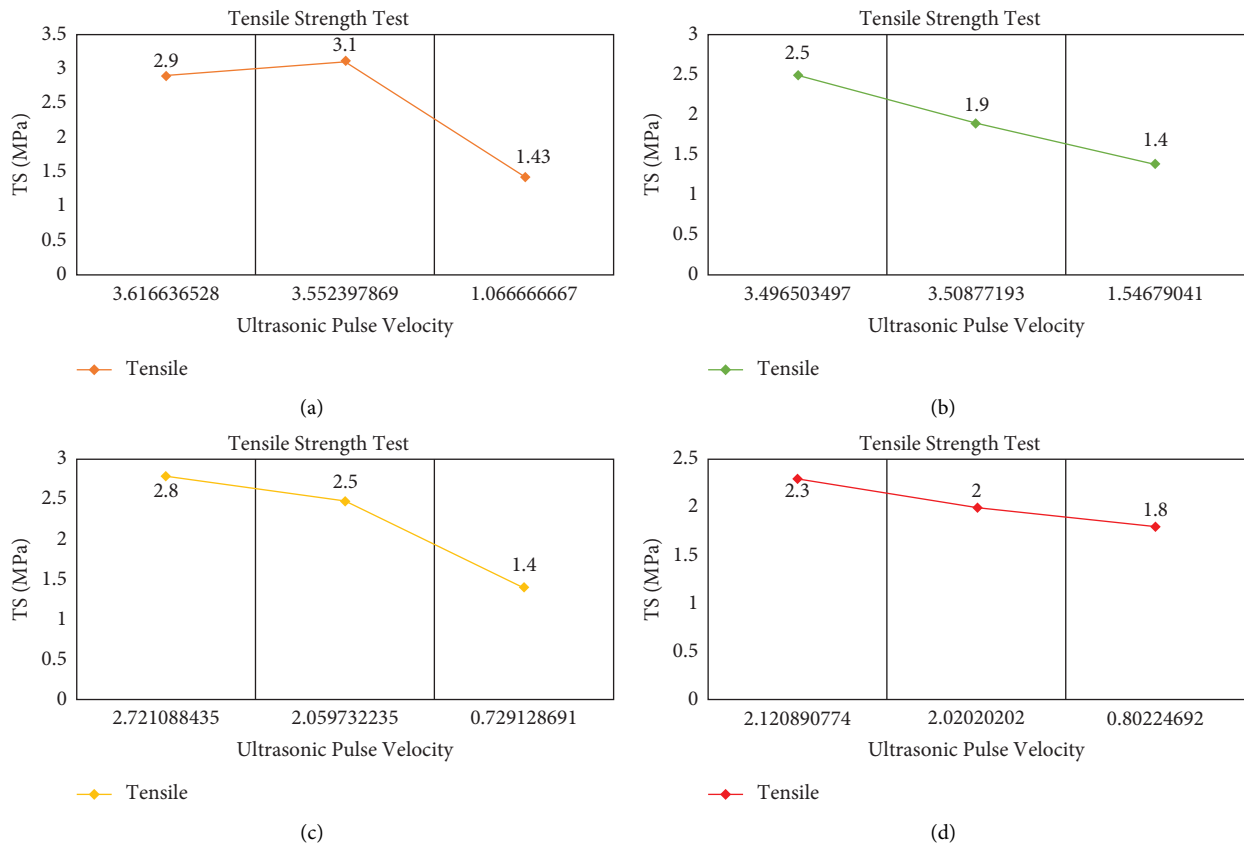

(a)

(b)

(c)

(d)

FIGURE 19: (a–d) Relationship between ultrasonic pulse velocity and tensile strength test of the concrete cylinder.

However, according to Subash et al [6] the findings in the article contradict the result of this test. In the study, high strength value was accounted for in the split tensile test for samples containing latex, 33.33% higher than the control sample; in this case, the inclusion of latex improved the tensile properties of the concrete. Figure 15 displays the comparison of the test result in this study to that of the

article, L1, L2, and L3 containing 4%, 5%, and 6% of latex to water ratio, respectively, M1, M2, and M3 containing 1%, 1.5%, and 2% of latex to concrete weight ratio.

The findings of the split tensile strength after heating at varying temperatures are shown in Figure 16, from this figure, the constant rise in temperature appears to have resulted in a similar decrease in split tensile strength in all
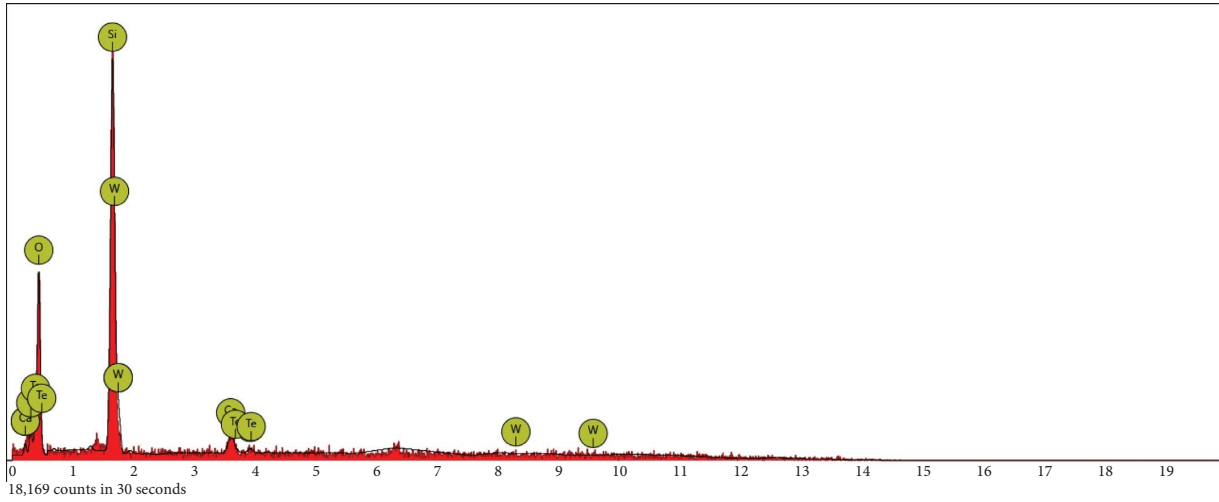
18,169 counts in 30 seconds

FIGURE 20: Graphical representation of elements concentration for control sample 800°C.

FIGURE 21: SEM for control sample 800°C.

38,572 counts in 30 seconds
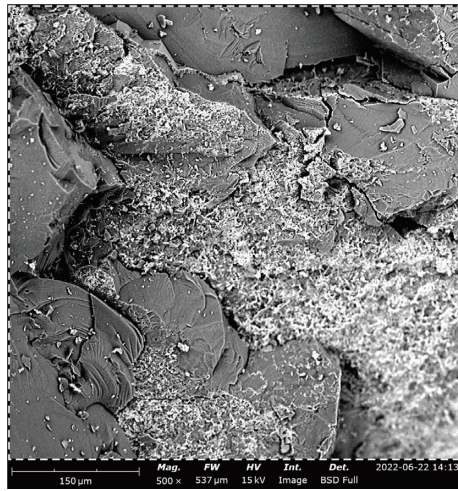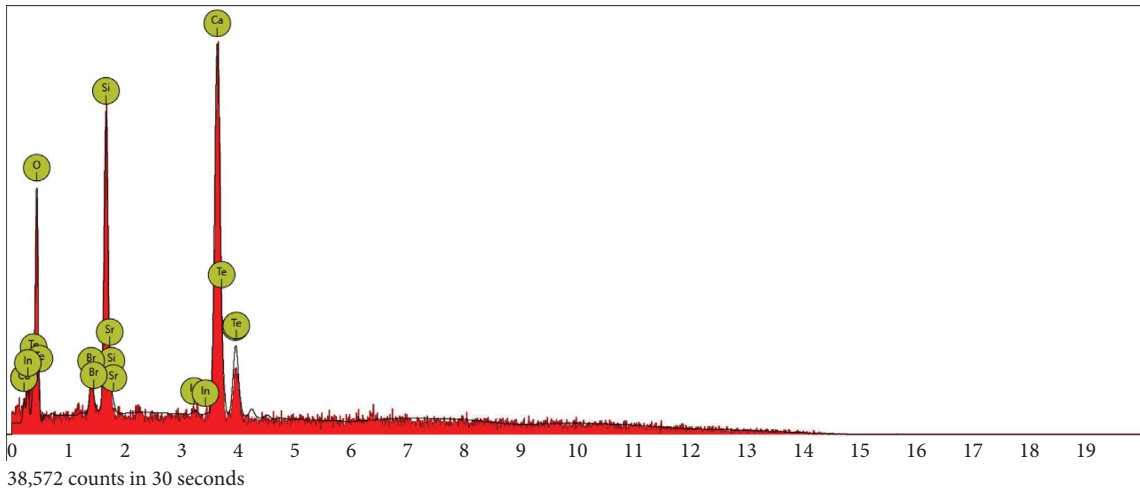
FIGURE 22: Graphical representation of elements concentration for the control sample.

Figure 23: SEM for the control sample.

64,477 counts in 30 seconds
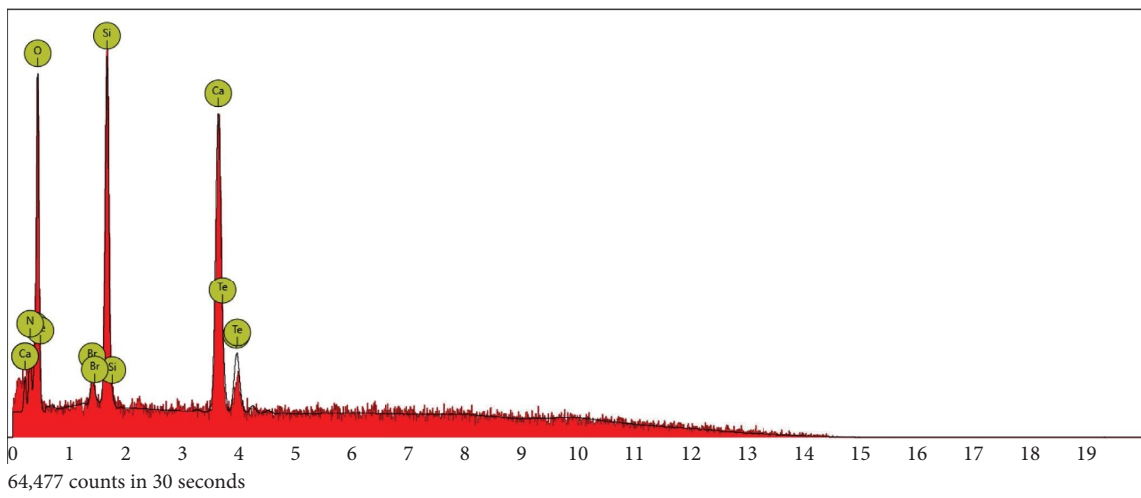
Figure 24: Graphical representation of elements concentration for M1 sample 800°C.

Figure 25: SEM for M1 sample.

82,397 counts in 30 seconds

FIGURE 26: Graphical representation of elements concentration for M1 sample room temperature.
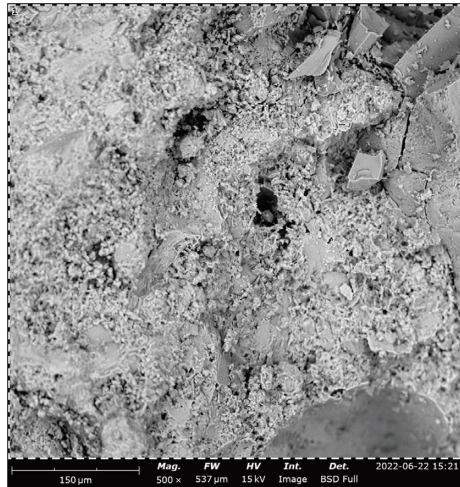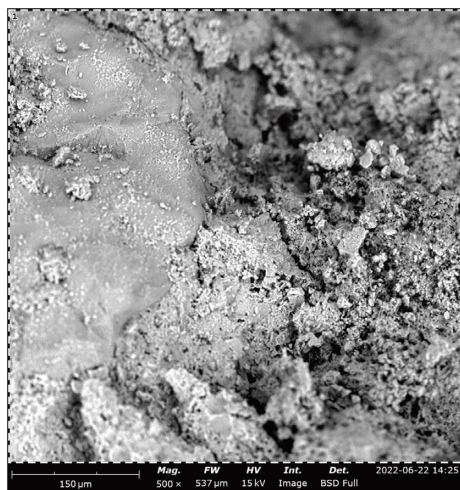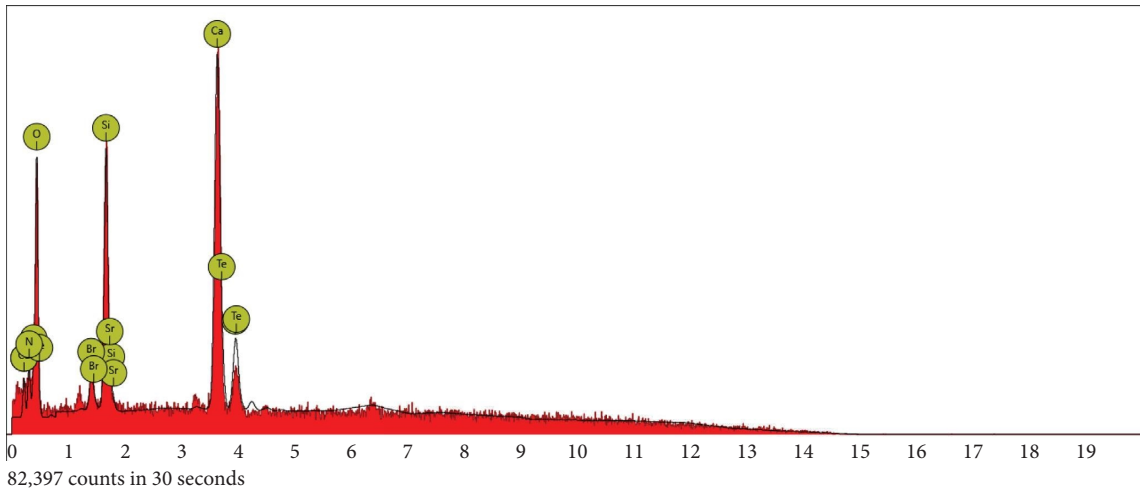

FIGURE 27: SEM for M1 sample room temperature.

23,444 counts in 30 seconds

FIGURE 28: Graphical representation of elements concentration for M2 sample 800°C.

FIGURE 29: SEM for M2 sample.

67,438 counts in 30 seconds
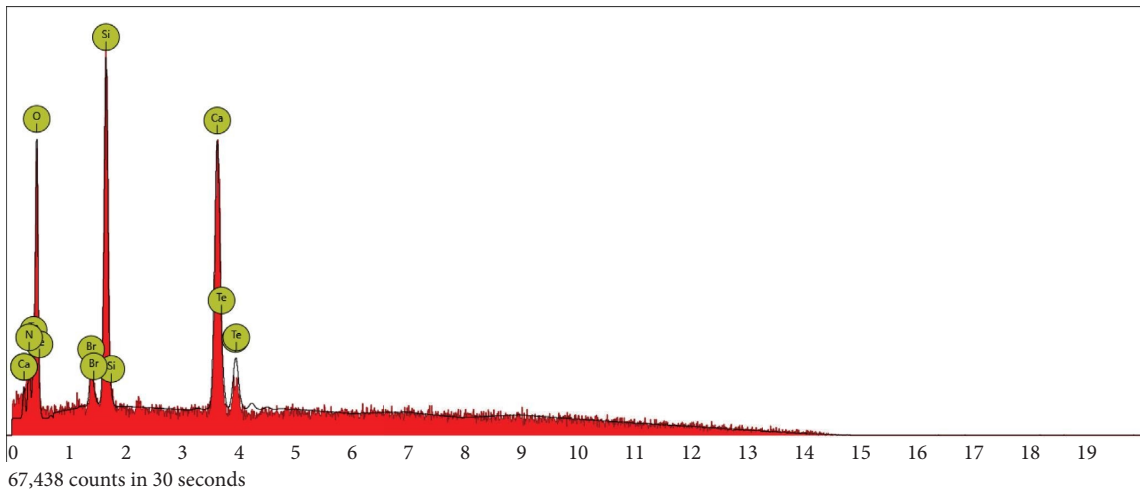
FIGURE 30: Element distribution in M2 sample at room temperature.

categories of concrete samples. From the data gotten from this test, the control sample performs best from 300°C to 800°C. At 300°C, the control sample has a split tensile strength of 2.9 N/mm^2, which accounts for the highest value in split tensile strength, while M3 accounts for the lowest split tensile strength of 2.3 N/mm^2. At 800°C, the control sample accounts for the highest split tensile strength value of 3.1 N/mm^2 and M1 accounts for the lowest split tensile strength value of 1.9 N/mm^2; the significant decrease in the split tensile strength of the M1 concrete sample is attributed to the percentage quantity of NRL added to the mix. At 1000°C, the decrease in strength of the control sample is noticeable, and it is due to the effects of elevated temperature, the M1 and M2 concrete samples have the same value of strength, and one could connote that the effects of temperature at 1000°C on concrete mix containing NRL dosage of 1% and 1.5% have the same level of strength. The M3 concrete sample shows superiority over the control
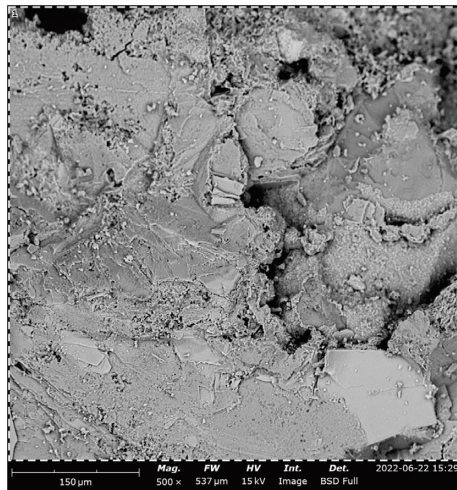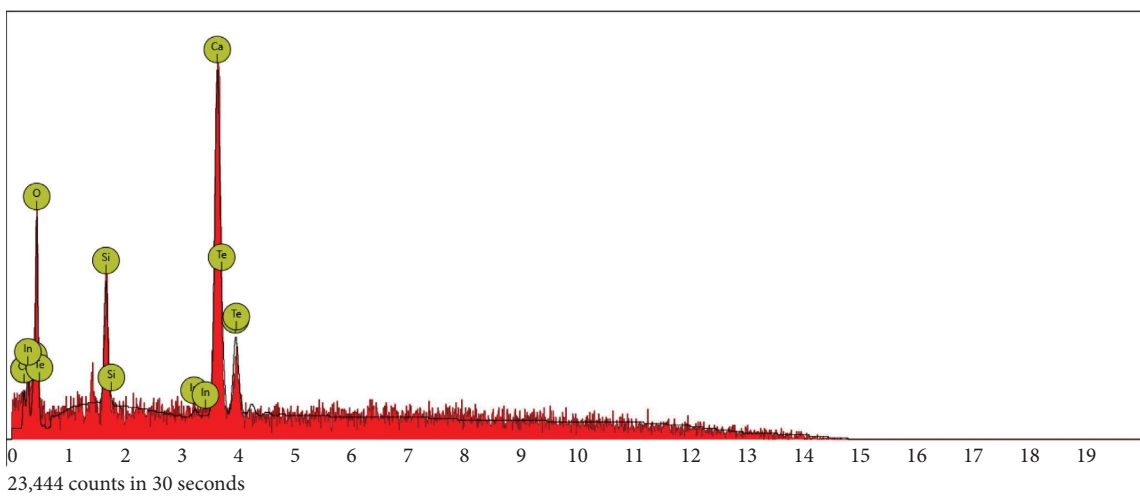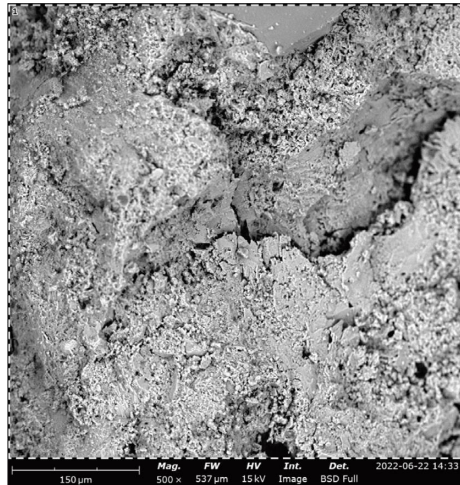

FIGURE 31: SEM for M2 sample.

Figure 32: Graphical representation of elements concentration for M3 sample 800°C.
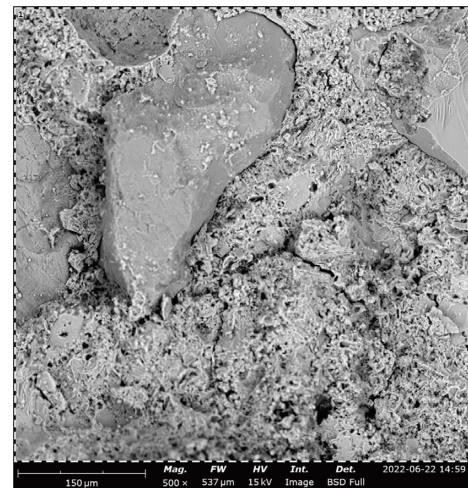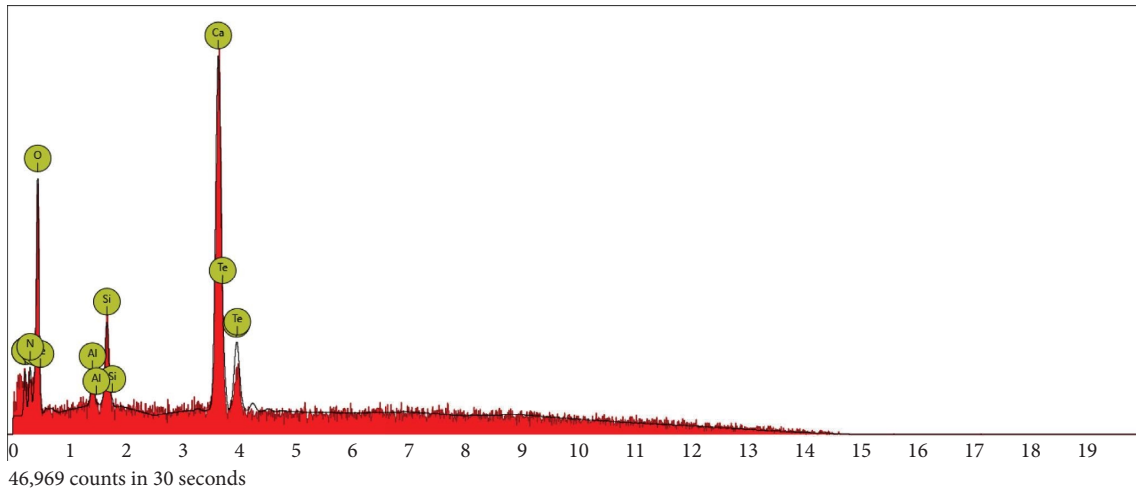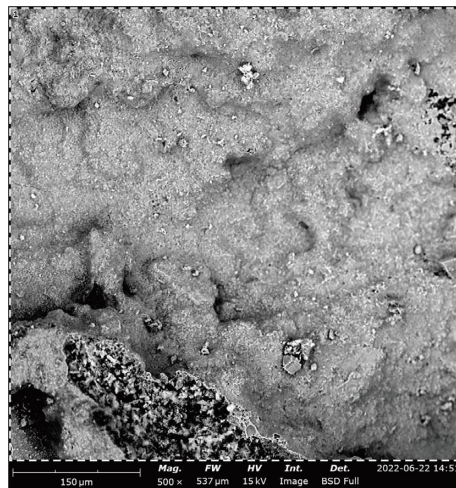

Figure 33: SEM for M3 sample.

sample having a split tensile strength of $1.8\,N/mm^2$, this indicates that at 1000°C the percentage quantity of NRL at 2% performs better than the rest this is attributed to latex film formation of NRL, 2% NRL provided a stronger elastic capability than other NRL dosages.

3.2.10. Rebound Hammer Test for Concrete Cylinder. Figure 17 gives the readings from the Schmidt hammer test carried out on the concrete cylinder. Looking at the behavior of the concrete samples and the rebound number value obtained at 300°C, the control sample containing 0% NRL recorded the highest value in the Schmidt hammer test with a rebound number value of 24, and the lowest rebound number was accounted for in M1 with a value of 16. This low

value in M1 is indicative of the poor quality of the concrete sample.

3.2.11. Ultrasonic Pulse Velocity for Concrete Cylinder. Based on the internal condition of the concrete cylinder, different times measured in Km/s may be required for the ultrasonic wave to travel through the concrete cylinder. The ultrasonic wave travels the longest to the opposite side of the concrete cylinder when the quality and integrity of the concrete cylinder are preserved, and it travels the shortest when the integrity has been influenced negatively. The Schmidt hammer test is carried out on the concrete cylinder after exposure to high temperature, the different concrete samples provide different values and travel time due to
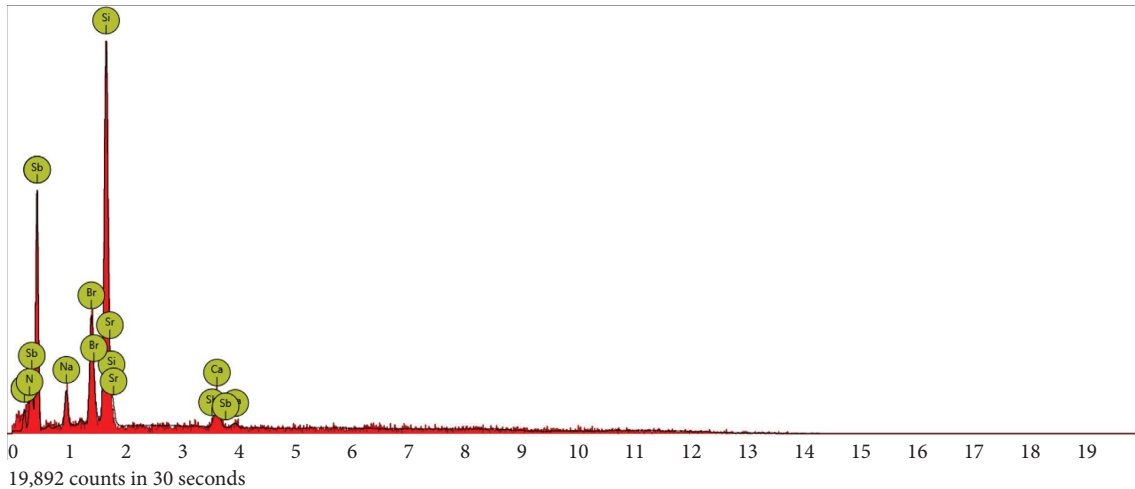
FIGURE 34: Graphical representation of elements concentration for M3 sample at room temperature.

varying temperatures, and the subjection of the concrete cylinder samples to varying temperatures of 300°C to 1000°C causing fractures or pores to be formed internally of the concrete samples, the effects of the formation of fractures and pores in the concrete cylinder led to shortening of the path which the ultrasonic waves will travel.

As seen in Figure 18, the time taken for the ultrasonic wave to travel through the concrete samples at 300°C is considerably high indicating the quality of the concrete cylinder at that temperature is considerably fair, although the control sample has the longest time of 3.6 km/s while the M3 sample has the shortest time of 2.1 km/s. At 800°C an increase in the travel time of ultrasonic wave in M1 is noticed due to the inclusion of NRL at a dosage of 1%; this implies that the inclusion of NRL at 1% affected the quality of the concrete sample positively and beyond that dosage seemed to only affect the quality of the concrete sample negatively. At 1000°C, qualities of the concrete cylinder have been nearly depleted the low travel time of the ultrasonic wave is indicative of that.

Figure 19 shows the relationship of ultrasonic pulse velocity and tensile strength test of concrete cylinder.

(1) Relationship of ultrasonic pulse velocity and tensile strength test of concrete cylinder is as follows:

  (a) Control sample
  (b) M1 Sample
  (c) M2 sample
  (d) M3 sample

3.2.12. Microstructural Analysis. For the microstructural analysis, a total of eight samples were considered for this test comprising of samples taken at room temperature and the samples subjected to 800°C for the four mixes. Figures 20–35 show the SEM-EDX for the tested samples. Comparing the samples taken at room temperature and at 800°C, the effect of temperature on the concrete matrix was significant as shown in the micrographs. At 800°C, the concrete surface appears firm than those taken prior to heating (room
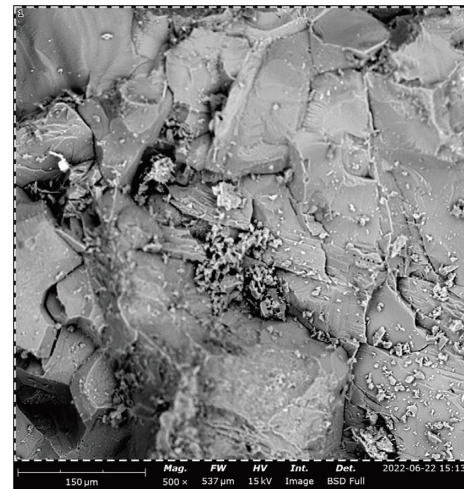
FIGURE 35: SEM for M3 sample.

temperature). As shown by the nondestructive test results, the well-dried samples due to heating gave higher rebound hammer number and UPVs. However, NRL addition at over 1% contributed to the inferior strength of the concrete, irrespective of the testing temperatures. Control Sample 800°C.

Control Room Temp.

(1) M1 sample 800°C

(2) M1 room temp

(3) M2 sample 800°C

(4) M2 sample room temperature

(5) M3 sample 800°C

(6) M3 room temperature

4. Conclusions

This study investigated the postfire residual strength and morphology of concrete incorporating natural rubber latex

exposed to elevated temperatures. The performance of the natural rubber latex-modified concrete in terms of workability and mechanical properties at room and varying temperatures was evaluated and compared to that of normal concrete. Also, the SEM-EDX of the NRL-modified concrete was analyzed. The following conclusions were drawn from the study:

(i) The workability of latex-modified concrete decreased with increasing dosage of rubber latex, and this resulted in the increasing viscosity of the fresh concrete

The post-fire strength of concrete showed a better performance in control concrete than the NRL-modified concrete. However, Mix M1 has appreciable strength at 800°C. The inclusion of rubber latex and with increasing percentage makes the concrete unstable when subjected to heating processes, and no form of improvement of the concrete is noted; the instability caused by the inclusion of the rubber latex is observed from the data obtained from the compressive strength of latex modified concrete.

(ii) Low split tensile and compressive strength values with fluctuations are noted in the latex-modified concrete, data obtained from the mechanical properties testing are inconsistent in comparison to that of normal concrete, which records the highest strength

(iii) The nondestructive tests performed, rebound hammer test and ultrasonic pulse velocity test, were higher in samples subjected to varying temperatures

Data Availability

The data used to support the findings of this study are included within the article.

Conflicts of Interest

The authors declare that they have no conflict of interest.

Acknowledgments

References

[1] S. K. Hirde and O. S. Dudhal, "Review on polymer modified concrete and its application to concrete structures," *International Journal of Engineering Research & Innovation*, vol. 4, no. 3, pp. 766–769, 2016.

[2] B. Georgali and P. E. Tsakiridis, "Microstructure of fire-damaged concrete. A case study," *Cement and Concrete Composites*, vol. 27, no. 2, pp. 255–259, 2005.

[3] M. Ismail, B. Muhammad, and N. A. Mohamad, "Durability performance of natural rubber latex modified concrete," *Malaysian Journal of Civil Engineering*, vol. 21, no. 2, 2009.

[4] B. Muhammad, M. Ismail, A. A. Yussuf, and A. R. B. Muhammad, "Elastomeric influence of natural rubber latex on cement mortar at high temperatures using thermal degradation analysis," *Construction and Building Materials*, vol. 25, no. 5, pp. 2223–2227, 2011.

[5] M. Ismail, B. Muhammad, A. A. Yussuf, Z. Majid, and M. E. Ismail, "Mechanical capabilities and fire endurance of natural rubber latex modified concrete," *Canadian Journal of Civil Engineering*, vol. 38, no. 6, pp. 661–668, 2011.

[6] S. Subash, K. M. Mini, and M. Ananthkumar, "Incorporation of natural rubber latex as concrete admixtures for improved mechanical properties," *Materials Today: Proceedings*, vol. 46, pp. 4859–4862, 2021.

[7] M. Sriring, A. Nimpaiboon, S. Kumarn et al., "Film formation process of natural rubber latex particles: roles of the particle size and distribution of non-rubber species on film microstructure," *Colloids and Surfaces A: Physicochemical and Engineering Aspects*, vol. 592, no. 2, Article ID 124571, 2020.

[8] P. Müller, J. Novák, and J. Holan, "Destructive and non-destructive experimental investigation of polypropylene fibre reinforced concrete subjected to high temperature," *Journal of Building Engineering*, vol. 26, Article ID 100906, 2019.

[9] Astm Standards, "Astm C150-07: standard specification for Portland cement," 2007, https://www.astm.org/standards/c150.

[10] P. C. Taylor, "Curing concrete," *Curing Concrete*, vol. 14, pp. 1–184, 2013.

[11] D. Y. Osei, Z. Mustapha, and M. D. Zebilila, "Compressive strength of concrete using different curing methods," *Journal of Social and Development Sciences*, vol. 10, no. 3, pp. 30–38, 2019.

[12] J. Suchorzewski and M. Nitka, "Size effect at aggregate level in microCT scans and DEM simulation–Splitting tensile test of concrete," *Engineering Fracture Mechanics*, vol. 264, Article ID 108357, 2022.

[13] P. K. S. Rathore, N. K. Gupta, D. Yadav, S. K. Shukla, and S. Kaul, "Thermal performance of the building envelope integrated with phase change material for thermal energy storage: an updated review," *Sustainable Cities and Society*, vol. 79, Article ID 103690, 2022.

[14] K. Kosugi and S. Kawahara, "Natural rubber with nanomatrix of non-rubber components observed by focused ion beam-scanning electron microscopy," *Colloid and Polymer Science*, vol. 293, no. 1, pp. 135–141, 2015.

[15] Is 13311 (Part-1), "Methods of non-destructive testing of concrete: Part-1: ultrasonic pulse velocity," 1992, https://www.iitk.ac.in/ce/test/IS-codes/is.13311.1.1992.pdf.

[16] A. Aseem, W. Latif Baloch, R. A. Khushnood, and A. Mushtaq, "Structural health assessment of fire damaged building using non-destructive testing and micro-graphical forensic analysis: a case study," *Case Studies in Construction Materials*, vol. 11, p. 258, 2019.

[17] H. R. Kumavat, N. R. Chandak, and I. T. Patil, "Factors influencing the performance of rebound hammer used for non-destructive testing of concrete members: a review," *Case Studies in Construction Materials*, vol. 14, p. 491, 2021.

[18] P. O. Awoyera and O. B. Olalusi, "Modeling temperature of fire-damaged reinforced concrete buildings based on

nondestructive testing and gene algorithm techniques," *Fire Technology*, vol. 58, no. 2, pp. 941–957, 2022.

[19] Z. S. Al-Khafaji, M. W. Falah, A. A. Shubbar et al., "The impact of using different ratios of latex rubber on the characteristics of mortars made with GGBS and Portland cement," *IOP Conference Series: Materials Science and Engineering*, vol. 1090, no. 1, Article ID 12043, 2021.

[20] M. Nibin Gafoor and P. R. Beena, *Effect of Natural Rubber Latex in concrete with Metakaolin Admixture: In Book - Recent Advances in Materials*, Mechanics and Management, Hamburg, Germany, 1 edition, 2019.

[21] F. Althoey, P. O. Awoyera, K. Inyama et al., "Strength and microscale properties of bamboo fiber-reinforced concrete modified with natural rubber latex," *Front. Mater.*vol. 9, Article ID 1064885, 2022.

[22] P. O. Awoyera, F. Althoey, H. Ajinomisan et al., "Potential of natural rubber latex in cement mortar for thermal insulating material in buildings," *Front. Mater.*vol. 10, Article ID 1152492, 2023.